Journal of Porous Materials
https://doi.org/10.1007/s10934-019-00773-3

Synthesis, characterization and antibacterial activity of imidazole-functionalized Ag/MIL-101(Cr)

Majid Hajibabaei[1] · Mostafa M. Amini[2] · Rezvan Zendehdel[1] · Mohamad Javad Nasiri[3] · Amir Peymani[4]

Abstract

Nowadays, nanomaterials have rapidly developed as a new generation of antibacterial agents. However, high local aggregation and concentration, and possible toxicity due to excess leaching are disadvantages of nanoparticles. Unique features of metal–organic frameworks (MOFs) such as coordinately unsaturated centers, high surface area and facile synthesis attracted attention to overcome the above-mentioned problems. In this context, Ag/MIL-101(Cr)/IMI was synthesized, and after characterization by powder X-ray diffraction (XRD), field emission scanning electron microscopy (FE-SEM–EDX), Transmission Electron Microscopy (TEM), Fourier-transform infrared spectroscopy (FTIR), inductively coupled plasma-optical emission spectrometry and BET surface area, TG–DTA was used as an antibacterial agent. Imidazole-functionalized Ag/MIL-101(Cr)/IMI presented a synergistic effect of imidazole and silver NPs against *Escherichia coli* (ATCC25292) and *Staphylococcus aureus* (ATCC25293) bacteria. The best antibacterial activity as minimum inhibitory concentration (MIC) was 6.2 µg/mL and 24.78 µg/mL of silver content against *E. coli* and *S. aureus*, respectively. There were 81 and 144.9 mg of Ag and imidazole per each gram of Ag/MIL-101(Cr)/IMI, which leaching rates of Ag, imidazole and Cr were 150, 828 and 153 µg/L, respectively. This leaching level of imidazole was lower than the amount recommended by Registry of Toxic Effects of Chemical Substances (RTECS) from NIOSH, while the leaching levels of silver NP and chromium is tended to be around the standard of WHO and U.S.EPA.

Keywords Post-synthetic strategy · MIL-101(Cr) · Silver nanoparticles · Imidazole · Antibacterial properties · Leaching

1 Introduction

Microbial contamination is one of the most problems in hospitals, medical equipment, and health care systems [1], food packaging and storage [2], textiles [3], water filtration equipment [4] and indoor air control systems [5, 6]. Nowadays, infection by microorganisms is becoming a serious and compelling subject for people's health. Infections threaten human life, while high costs impose on societies [1, 7]. However, preparation of a new antimicrobial agent by the potential biofunctional antibacterial strategy is essential to produce the biocidal materials [8, 9].

Metals such as Ag, Zn, and Cu and metal oxides such as ZnO, Cu_2O and CuO nanoparticles are very well known compounds as antibacterial agents [10, 11]. Silver NP is one of the best metals with high antibacterial efficiency in the sizes less than 30 nm and less toxicity than many other nanomaterials [10, 12–14]. But the use of silver NP is limited due to nanoparticles aggregation, low stability, the release of metal ions from media and indirect/direct toxicity [15].

Electronic supplementary material The online version of this article (https://doi.org/10.1007/s10934-019-00773-3) contains supplementary material, which is available to authorized users.

✉ Rezvan Zendehdel
zendehdel76@yahoo.com

[1] Department of Occupational Hygiene, School of Public Health and Safety, Shahid Beheshti University of Medical Sciences, Tehran, Iran

[2] Department of Chemistry, Shahid Beheshti University, G.C., P.O. Box 19396-4716, Tehran, Iran

[3] Department of Medical Microbiology, School of Medicine, Shahid Beheshti University of Medical Sciences, Tehran, Iran

[4] Medical Microbiology Research Center, Qazvin University of Medical Sciences, Qazvin, Iran

Published online: 31 May 2019

One way to overcome these problems is to immobilize the nanoparticles on the porous material such as silica, zeolite, etc. [16, 17]. Moreover, the decrease of silver leaching to a lower level than the health and environmental standards without a change in antibacterial properties and maintaining them in the long term is an important task [18, 19].

One of the candidate compounds for metal immobilizing is metal–organic frameworks (MOFs). These porous coordination polymers made up of various organic bridging ligands and metal ions and have large surface areas and high porosity [20–22]. MOFs are one of the most important porous materials that have been used extensively in many cases such as separation [23], heterogeneous catalysis [24], sensing [25, 26] and drug release [27], adsorption [28–30] and air purification [31, 32].

The antibacterial activities of MOFs have been reported in several studies [33–37]. MIL-101(Cr) is a MOF which has large cavities (more than 30 Å) with coordinatively unsaturated sites (CUSs). There are suitable properties such as high thermal, chemical, and solvent stability in MIL-101(Cr) for connecting to functionalized groups [38–41]. Post-synthesis modification of MOFs by incorporation of metal ions and organic molecules is a suitable approach to improve MOFs properties [38, 42–45].

N-alkylated imidazole appears to promise a potential to use as an antibacterial and antifungal agent [46–48]. On the other hand, embedding imidazole into the pore spaces of MOFs increases the concentration of protons [49–52]. The positive surface charge of antibacterial materials is important for bacterial adhesion [53]. The positively charged grafted onto the MIL-101(Cr) surface by imidazole confers electrostatic attraction between imidazole functionalized MIL-101(Cr) and negatively charged surface of bacteria [54, 55].

Research motivation in this study was to understand the synergistic effect between silver NPs and imidazole as a bactericidal. In this context, antibacterial activities of MIL-101(Cr), Ag/MIL-101(Cr), and MIL-101(Cr)/IMI have been investigated and results compared with antibacterial activity of Ag/MIL-101(Cr)/IMI.

2 Materials and methods

2.1 Chemicals and materials

All solvents and reactants, including chromium(III) nitrate nonahydrate ($Cr(NO_3)_3{\cdot}9H_2O$, 99%), terephthalic acid ($C_6H_4(COOH)_2$, 98%), silver nitrate ($AgNO_3$, 99%), sodium borohydride ($NaBH_4$, 96%), ethanol (C_2H_5OH, pure), anhydrous toluene ($C_6H_5CH_3$, 99.8%), acetone (CH_3COCH_3, pure), *N*,*N*-dimethylformamide ($(CH_3)_2CHO$, 99.8%), imidazole ($C_3H_4N_2$, 99%) were commercially purchased from either Sigma-Aldrich or Merck Chemical and used without further purification. Both Mueller–Hinton broth and blood agar (TSA) were also procured from Merck.

2.2 Materials characterization

Powder X-ray diffraction (XRD) patterns were recorded on a STOE diffractometer with the operating power of 40 kV/40 mA, and the diffraction data were collected between 5° and 80° (2θ) using the Cu Kα radiation (λ = 1.5418 Å). FE-SEM (TESCAN/MIRA3) and TEM (Philips CM30) operating at 200 kV were employed to determine the Ag/MIL-101(Cr)/IMI morphology and particle size. The size distribution of silver NPs were calculated using the Image software.

BET surface area measurements were conducted using a BELSORP-mini II (BEL Japan) apparatus at liquid nitrogen temperature (77 K). The sample was degassed at 423 K for 3 h and surface areas were calculated using the BET equation between $P/P_0 = 0–0.05$. The total pore volume was carried out by a single point method at $P/P_0 = 0.984$.

Ag content of Ag/MIL-101(Cr)/IMI and the leaching of Ag and Cr from post-synthesized MOF were analyzed by inductively coupled plasma optical emission spectrometry (Vista pro, Varian) and elemental analyses (for C/H/N) were determined using Elemental CHNS Analyzer Vario El III analyzer. Fourier transform infrared (FTIR) spectra (WQF-510A) were obtained with KBr disks in 400–4000 cm^{-1}. Thermal analysis (TG–DTA) was conducted on a Bahr STA-503 instrument. The leaching of imidazole was determined by HPLC–MS (MODEL: Waters Alliance 2695 HPLC-Micromass Quattro Micro API Mass Spectrometer).

2.3 Synthesis of MIL-101(Cr) nanoparticles

MIL-101(Cr) was hydrothermally synthesized according to Bromberg et al. method [56]. Briefly, chromium (III) nitrate nonahydrate (10 g), terephthalic acid (4.15 g), and deionized water (100 mL) were mixed and put in a 500 mL Teflon-lined autoclave. Then autoclave was heated at 218 °C for 18 h without stirring. After cooling autoclave to ambient temperature, the suspension was centrifuged to separate the green solid of MIL-101(Cr) from the water. This sediment was washed with water, methanol and acetone. Powder of MIL-101(Cr) was placed in *N*,*N*-dimethylformamide (100 mL) and was sonicated for 10 min and then kept overnight at 70 °C. The product was washed with methanol and acetone. Finally, it was activated at 150 °C under vacuum for 12 h.

2.4 Synthesis of Ag/MIL-101(Cr)/IMI

Scheme 1 shows the strategy for the preparation of imidazole-functionalized Ag/MIL-101(Cr), which adapted from Cao et al. report [57]. Briefly, activated MIL-101(Cr) (1.0 g) was immersed in deionized water (40 mL) containing silver nitrate (250 mg) and was stirred for 14 h at room temperature (25% w/w). Next, the suspension was dried under the vacuum for 2 h at 100 °C. Finally, Ag^+ was reduced to Ag^0 by 4 mL of 1.7 mmol/mL $NaBH_4$ (250 mg), while it was agitated at room temperature for 1 h.

For the preparation of imidazole-functionalized MOF (MIL-101(Cr)/IMI), 1.0 g of activated MIL-101(Cr) was suspended in 100 mL of anhydrous toluene and then imidazole (100 mg) was dissolved in anhydrous toluene (10 mL) and added to the slurry dropwise. This blend was refluxed at 120 °C for 15 h with continuous stirring [38]. The product was centrifuged and then washed with ethanol and deionized water. Finally, the product was dried in a vacuum oven at 80 °C for 4 h to yield MIL-101(Cr)/IMI. Ag/MIL-101(Cr)/IMI was prepared similarly using Ag/MIL-101(Cr).

2.5 Antibacterial activity tests

Antibacterial activity tests of the Ag/MIL-101(Cr), MIL-101(Cr)/IMI and Ag/MIL-101(Cr)/IMI were performed

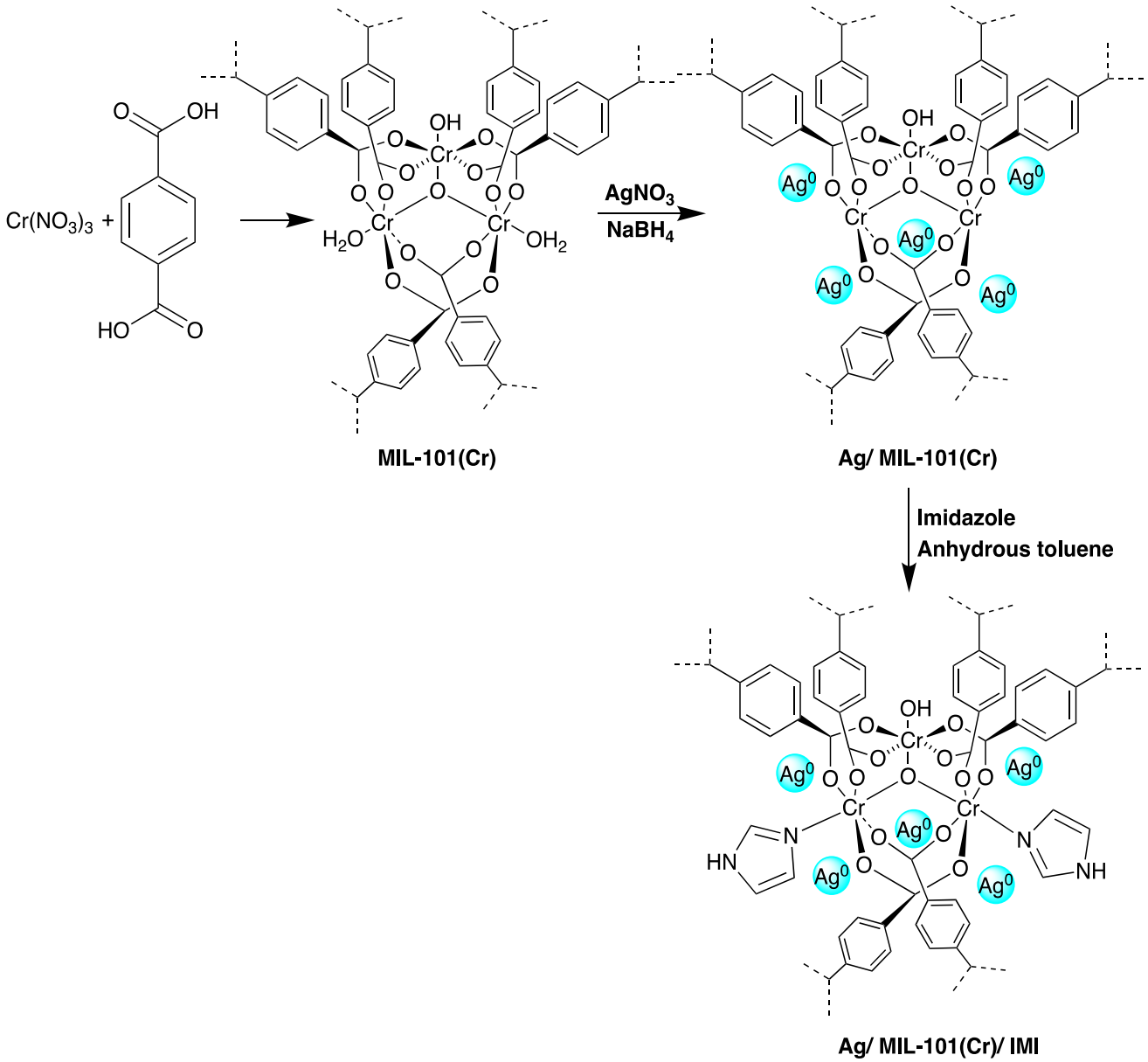

Scheme. 1 Synthesis of Ag/MIL-101(Cr)/IMI antibacterial agent from MIL-101(Cr), imidazole and silver NP

against the Gram-positive *Staphylococcus aureus* ATCC 25923 (*S. aureus*) and Gram-negative *Escherichia coli* ATCC 25922 (*E. coli*). Reference strains were purchased from Padtanteb Co. in Iran. Strains of *E. coli* and *S. aureus* were inoculated into Mueller–Hinton broth to culture the bacteria at 37 °C for 20 h. Moreover, fresh bacteria were incubated on the blood agar plates at 37 °C for 20 h. Minimum inhibitory concentration (MIC) and minimum bactericidal concentration (MBC) levels of post-synthesized MIL-101(Cr) were evaluated according to CLSI recommendations [58]. Briefly, stock concentrations of 320 mg/mL from the compounds were prepared in sterile distilled water and 0.5% dimethylsulfoxide (DMSO). The concentrations of the working solutions were selected around 16 dilutions between 80 mg/mL and 2.25 µg/mL. The colonies were touched with a loop; the loop was then suspended in 0.9% saline solution, and the turbidity of the bacterial suspension was adjusted to 0.5 McFarland standard. The suspension was subsequently diluted 1 in 50 where the concentration of bacteria was nearly 10^6 CFU/mL. Sterile Mueller–Hinton broth (100 µL) was added to all wells of a 96-well plates; 100 µL of synthesized agents were then added to the two rows of each plate, and 1:2 serial dilutions were prepared in each column of wells. The final concentration was between 1×10^5 and 1×10^6 CFU/mL in the 96-well plates. Then, the microplates were placed in an incubator at 37 °C for 20 h. Gentamicin (10 mg/mL) was used as a positive control, for each bacterial strain. A growth control (without synthesized agents) and a sterile control (without bacteria) were also included. To determine the MBC and MIC levels, 15 µL aliquots were taken from the wells; were plated on Mueller–Hinton agar plates and were then incubated for 24 h at 37 °C. The lowest concentration of chemicals that destroyed 99.9% of the initial bacteria was considered as MBC, while the MIC was determined as the lowest concentration of the agent which inhibited the growth of them. Each test was repeated in at least triplicate.

2.6 Silver and imidazole leaching from Ag/MIL-101(Cr)/IMI

First, 21 mg of Ag/MIL-101(Cr)/IMI was poured into 100 mL of distilled water. Next, the prepared sample was stirred for 24 h at 120 rpm using a magnetic mixer. Finally, 5 mL of supernatant was analyzed by ICP-OES for Ag and chromium and HPLC–MS for imidazole leaching.

3 Results and discussion

3.1 Characteristics of nanoparticles

Powder X-ray diffraction patterns of MIL-101(Cr), Ag/MIL-101(Cr) and Ag/MIL-101(Cr)/IMI are shown in Fig. 1. As can be seen, the XRD patterns of Ag/MIL-10(Cr) and Ag/IMI/MIL-10(Cr) are consistent with the XRD pattern of MIL-101(Cr) which indicate the framework structure of MIL-101(Cr) after doping with silver and also after treating of post-synthesized Ag/MIL-101(Cr) with imidazole has been preserved. Further, the appearance of well-shaped diffractions at 2Θ of 38°, 44°, 64°, and 77° demonstrate the presence of silver NPs in MIL-101(Cr) [59, 60]. Also, FTIR spectrum of MIL-101(Cr) in the range of 1600–500 cm^{-1} (Fig. 1S) with well define stretching vibration band of Cr–O at 570 cm^{-1} confirm that the structure of MIL-101(Cr) remained intact after loading silver and treating with imidazole [61]. Furthermore, the bands at 2925 and 1051 cm^{-1} in FT-IR spectrum of Ag/MIL-101(Cr)/IMI have been assigned to the aliphatic C–H, and C–N stretching vibrations, respectively [38, 39], and unambiguously indicate the presence of imidazole in target compound.

Figures 2 and 3 shows the FESEM and TEM images of the Ag/MIL-101(Cr)/IMI nanocrystal. The particle size of Ag/MIL-101(Cr)/IMI was in the range from 150 to 253 nm. The mean diameter of Ag nanoparticles from TEM image was determined to be 11.34 ± 3.85 nm (Fig. 3). Interestingly, there is a uniform distribution of the selected particles length in EDS mapping and line scan of Ag/MIL-101(Cr)/IMI where Ag is located in the internal core structure along with C, O, Cr elements and imidazole (N) is placed in the external shell (Figs. 2S and 4). Moreover, N and Ag signals

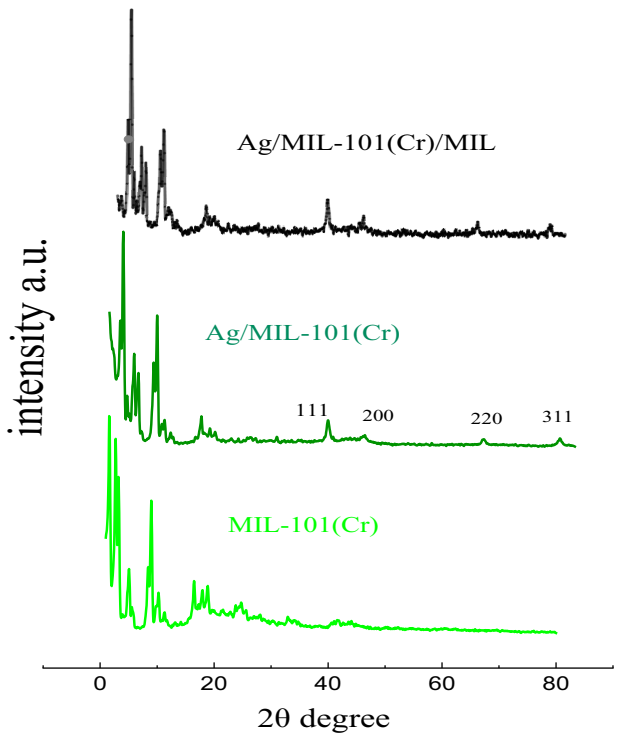

Fig. 1 X-Ray diffraction patterns of MIL-101(Cr), Ag/MIL-101(Cr) and Ag/MIL-101(Cr)/IMI

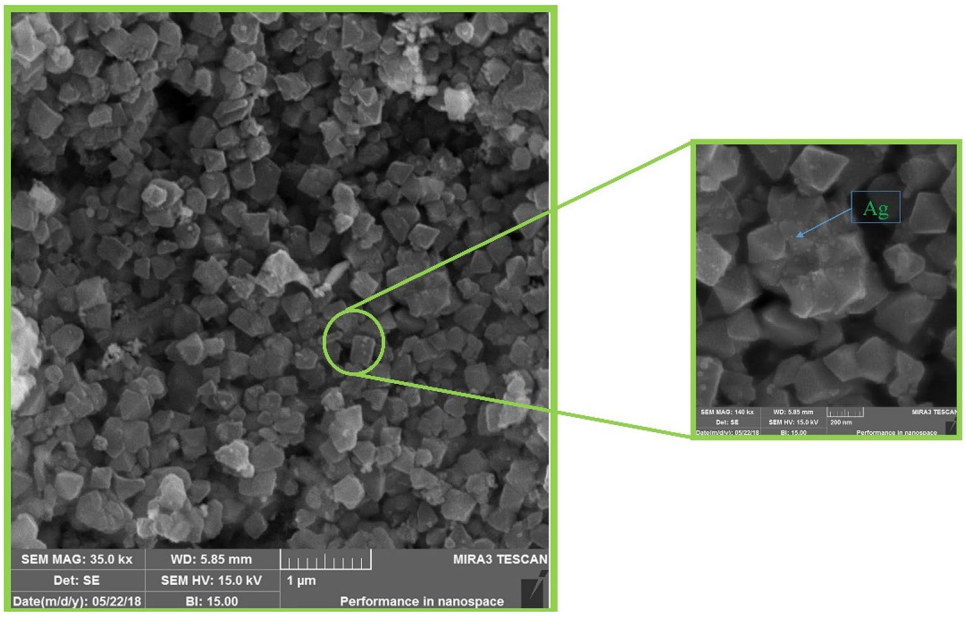

Fig. 2 FE-SEM image of Ag/MIL-101(Cr)/IMI

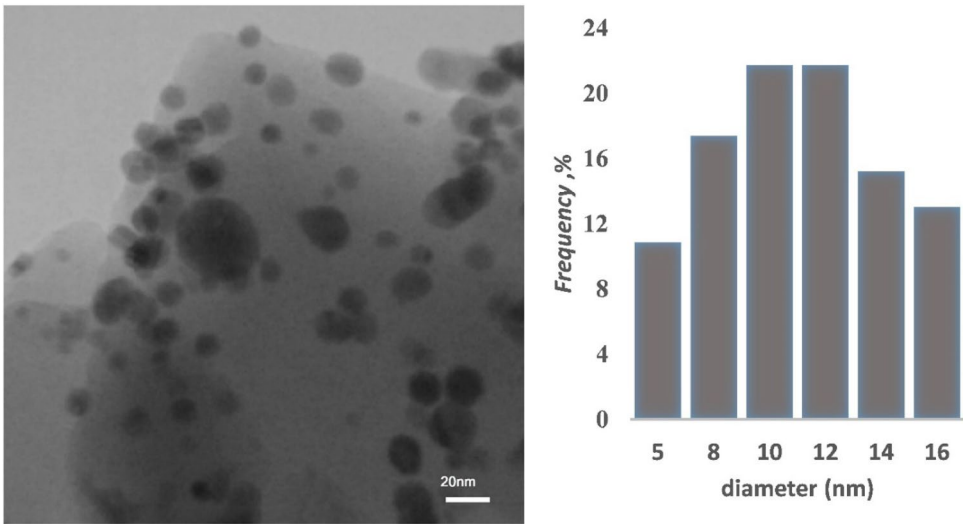

Fig. 3 TEM images of Ag/MIL-101(Cr)/IMI and the size distribution of Silver NPs

at 0.3 and 2.5 keV confirm the existence of N and Ag elements in Ag/MIL-101(Cr)/IMI crystal [16, 62].

Nitrogen adsorption–desorption isotherms exhibit that surface area and total pore volumes of Ag/MIL-101(Cr)/IMI have declined compared to those of MIL-101 (Cr). BET surface area of nanocrystal decreased from 1835 to 426 m^2/g (Fig. 5) and total pore volumes declined from 0.87 to 0.258 cm^3/g [63]. Therefore, it was concluded that the pores of MIL-101(Cr) were not significantly closed after silver doping and imidazole-functionalizing, while significant reduction has been reported in the surface area and the pore volume of amine-functionalized zeolite NaY [54]. Thermal analysis was conducted to study the stability of the Ag/MIL-101(Cr)/IMI. As TG curve in Fig. 6 shows, there is about 40% mass loss from 350–550°C. This mass loss is accompanied by exothermic peaks in the DTA curve in the same temperature and indicates a rapid decomposition of the Ag/MIL-101(Cr)/IMI, therefore, it can be concluded that the prepared nanoparticles thermally are stable up to 380 °C.

Table 1 lists the amount of doped silver and imidazole in different MIL-101(Cr) post-synthetized compounds. The level of Ag-doped in Ag/MIL-101(Cr)/IMI nanoparticles assessed to be 8.1% according to ICP-OES analysis. To determine the amount of imidazole in Ag/MIL-101(Cr)/IMI, its nitrogen content was determined by CHNS Elemental Analyzer. The amount of nitrogen was 5.96 wt%. Therefore, it can be concluded that imidazole loading was 14.49 wt% in combination with C, 31.49%; H, 2.7% and C/N ratio, 5.28.

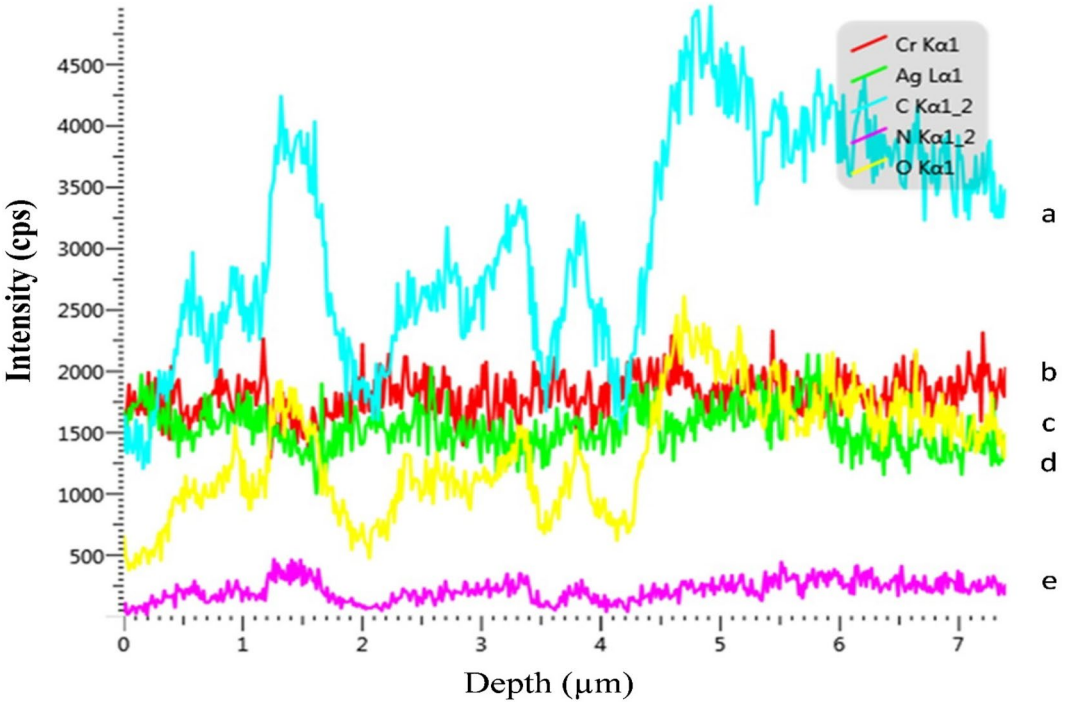

Fig. 4 Line-scan EDX in an area; (a) (carbon), (b) (chrome), (c) (oxygen), (d) (silver), (e) (nitrogen)

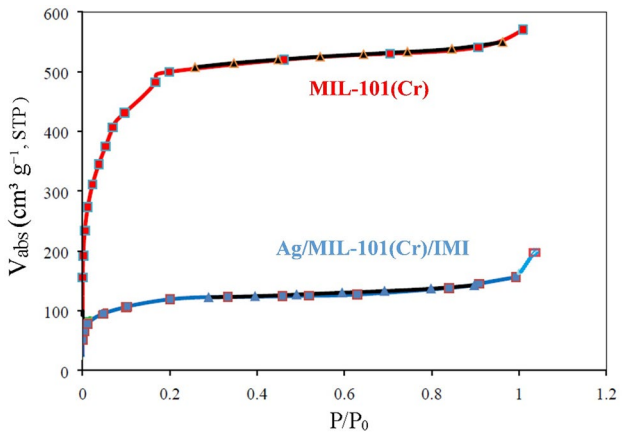

Fig. 5 N_2 adsorption–desorption isotherms at 77 K for MIL-101(Cr), Ag/MIL-101(Cr)/IMI

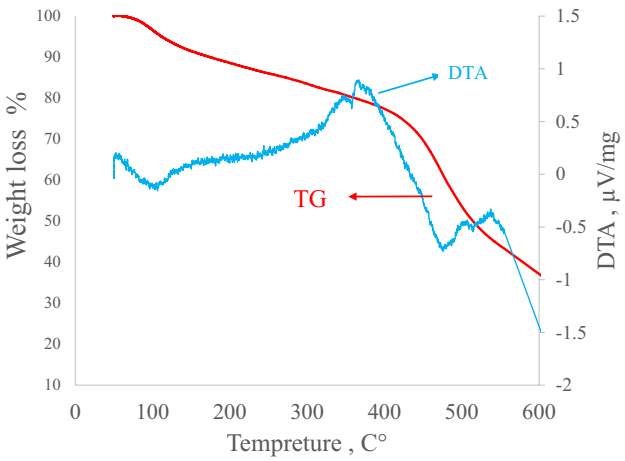

Fig. 6 TG-DTA profile of Ag/MIL-101(Cr)/IMI

3.2 Leaching of silver and imidazole

The amount of Ag leaching in distilled water was measured to be 0.714 mg from 1.0 g of Ag/MIL-101(Cr)/IMI, while 81 mg of Ag has been doped to 1.0 g of post-synthesized MOF. The percentage of silver leaching from Ag/MIL-101(Cr)/IMI (0.88%) is lower than the reported leaching of similar studies [18, 54, 64]. The silver leaching rate in this study was 150 μg/L, while a leaching limit of 100 μg/L has been recommended by the World Health

Table 1 Percent of doped agents in different MIL-101(Cr) post synthetized compound

Compound	Ag	Imidazole
Ag/MIL-101(Cr)	13.7	–
MIL-101(Cr)/IMI	–	15.55
Ag/MIL-101(Cr)/IMI	8.1	14.49

Organization (WHO) in bacteriostatic agents [65]. The level of 144.9 mg of imidazole was assessed in 1.0 g of Ag/MIL-101(Cr)/IMI, while 3.94 mg (2.72%) was leached for each 1.0 g of Ag/MIL-101(Cr)/IMI. According to the Registry of Toxic Effects of Chemical Substances (RTECS) from NIOSH, DNA inhibition in humans by imidazole occurs in 68 mg/L, while imidazole leaching was 0.828 mg/L in this study [66]. It seems that the leaching of imidazole from Ag/MIL-101(Cr)/IMI is lower than the limit level of health. The chromium leaching rate was measured to be 153 µg/L for Ag/MIL-101(Cr)/IMI, while a limit of 50 and 100 µg/L have been recommended for drinking water by the WHO and the U.S.EPA, respectively [67, 68]. Based on the EDS mapping, elemental Ag and imidazole locate in the internal core and external shell, respectively, which affect the reduction of leaching process. However, imidazole can be substituted with water (or OH) molecules providing the coordinately unsaturated sites (CUSs) of Ag/MIL-101(Cr). Consequently, this produces the strong interactions between imidazole and Ag/MIL-101(Cr) which leads to minimizing the leaching of imidazole [40]. Since the XRD pattern of Ag/MIL-101(Cr) after introducing imidazole did not change therefore, it can be concluded that Ag and imidazole interaction did not take place. Such a low silver leaching can be attributed to the low solubility of elemental silver in aqueous solution.

3.3 Antibacterial activity

The main aim of this study was to prepare a suitable antibacterial nanoparticle with good antibacterial activity and low leaching rate. To achieve this goal, imidazole and silver with antibacterial properties [13, 46] were selected. In the other hand, the surface area and the pores in the MIL-101 are large enough to embed imidazole and silver NP [69]. Therefore, Ag/MIL-101(Cr)/IMI was synthesized and its antibacterial activity was evaluated by the MIC/MBC techniques against *E. coli* and *S. aureus* bacteria.

Inhibition strengths of different nanoparticles are shown in Fig. 3S. The results of Table 2 shows that the MIC of MIL-101(Cr) is 20 mg/mL for *E. coli* in MIL-101(Cr). In a similar report, MIC result of Commercial Cu-BTC has been 64 mg/mL for *E. coli* [70]. The MIC of *E. coli* decreased from 20 to 0.3 mg/mL in Ag/MIL-101(Cr).

The results of Table 2 suggest that, in addition to reducing the values of MIC/MBC by silver NP, imidazole-functionalized also enhances the antibacterial activity of MIL-101(Cr). The remarkable point is that silver NP and imidazole have a synergistic effect, which has been presented in the antibacterial potency of Ag/MIL-101(Cr)/IMI.

It should be noted that the reduction of the silver ion (Ag^+) to the elemental Ag in zeolite decreases the antibacterial activity [71]. The antimicrobial activity of Ag/MIL-101(Cr)/IMI (MIC; 0.076 mg/mL, 8.1 wt% Ag) is comparable with that of Ag^+/zeolite (MIC; 0.2 to 0.5 mg/mL, 9.8 wt% Ag) reported by Ferreira et al. [72, 73] despite the reduction of the silver. Consequently, Ag^+ is released slower than Ag^+ led to an increase in the bactericidal activity of Ag/MIL-101(Cr)/IMI in the long term [18]. Therefore, it can be concluded that the antibacterial activity of Ag/MIL-101(Cr)/IMI is preferred to ion-exchanged zeolite due to higher host potency as well as lower leaching efficacy. Silver NPs based MOFs by Lu et al. were demonstrated to have antibacterial activity with MIC of 5–15 µg/mL and leaching of Ag was 18.76–25.1 ppm while leaching rate of silver was 0.15 ppm in this work [74].

Table 2 Minimal inhibitory concentration (MIC) and minimal bactericidal concentration (MBC) results in mg mL^{-1} of antibacterial agent

	E. coli		*S. aureus*	
	MIC	MBC	MIC	MBC
MIL-101(Cr)	40	80	80	160
MIL-101(Cr)/IMI	20	40	40	80
Ag/MIL-101(Cr)	0.306	0.612	0.612	1.225
Ag/MIL-101(Cr)/IMI	0.076	0.153	0.306	0.612
Gentamicin	0.0005	0.001	0.009	0.018

Mortada et al. prepared postmetalated MOFs and tested it against *E. coli*. MIC of UiO-67-bpdc-Ag was 50 µg/mL which is equivalent to 6.5 µg/mL of silver content with 0.85% of the silver leached [75]. The MIC of 6.2 µg/mL of silver content with 0.88% of the silver leaching reported in this research. It is necessary to mention, the mass ratio of the MOF/$AgNO_3$ in the synthesis of UiO-67-bpdc-Ag was 1:2 [75], but in this work, the mass ratio for the synthesis of Ag/MIL-101(Cr)/IMI is 1:4 which indicated less $AgNO_3$ consumption. Erchel et al. investigated the antibacterial activity of Ag3(3-phosphonobenzoate) for *E. coli* with a reported MIC of 50 µM and leaching of at least 1.2% [76].

Imidazole-functionalized not only has intrinsic antibacterial activity but also increases the protons conductivity of Ag/MIL-101(Cr) [51, 52]. This potency could increase the antibacterial activity due to electrostatic attraction between the positively charged surface of the Ag/MIL-101(Cr) and negatively charged membranes of bacteria, which lead to adhesion of bacteria to the supporter surface [53]. As stated in various reports [55, 77], biocidal mechanisms of nanoparticles can be summarized as follows: (1) Adhering of the bacterial cell membrane to the surface of media; (2) Penetrating inside the cells and disruption in the intracellular organizations; (3) Free radicals and reactive oxygen species (ROS) generation. The TEM results of Ag/MIL-101(Cr)/IMI show that the mean diameter of silver NPs were 11.34 nm. Therefore, it can be concluded that a smaller silver NP enters the bacteria directly and can boost the generation of free

radicals, causing stronger antimicrobial activity according to previous studies [78, 79].

The results of this study show that *S. aureus* is less susceptible to Ag/MIL-101(Cr)/IMI than *E. coli* bacteria. It could be related to the thickness of the cell membrane, whereas the peptidoglycan layer of G^+ bacteria is thicker than G^- types. Many similar studies confirm the findings of the present research [80, 81].

4 Conclusion

Overall, in this work, Ag/MIL-101(Cr)/IMI was first synthesized as a proper nanoparticle for antibacterial applications. The post-synthesis of MIL-101(Cr) with imidazole and silver NP led to an outstanding synergistic effect of antibacterial activity towards different pathogens including *E. coli* and *S. aureus*. Ag/MIL-101(Cr)/IMI showed much better MIC/MBC values than Ag/MIL-101(Cr). Also, this study presented that in spite of the limited leaching of silver and imidazole from Ag/MIL-101(Cr)/IMI, the antibacterial activity is at a desirable level. The leaching levels of silver NP and chromium is tended to be around the standard of WHO and EPA, while the leaching level of imidazole was lower than the level recommended by RTECS from NIOSH organization.

Acknowledgement This research was part of a PhD thesis and financially supported by the School of Public Health and safety, Shahid Beheshti University of Medical Sciences (Grant No. IR.SBMU.PHNS.REC.1396.58).

References

1. A.Y. Peleg, D.C. Hooper, N. Engl. J. Med. **362**, 1804 (2010)
2. P. Appendini, J.H. Hotchkiss, Innov. Food Sci. Emerg. Technol. **3**, 113 (2002)
3. R. Dastjerdi, M. Montazer, Colloids surf. B **79**, 5 (2010)
4. Q. Li, S. Mahendra, D.Y. Lyon, L. Brunet, M.V. Liga, D. Li, P.J.J. Alvarez, Water Res. **42**, 4591 (2008)
5. B. Flannigan, R.A. Samson, J.D. Miller, *Microorganisms in home and indoor work environments: diversity, health impacts, investigation and control* (CRC Press, Boca Raton, 2002)
6. S.C. Verde, S.M. Almeida, J. Matos, D. Guerreiro, M. Meneses, T. Faria, D. Botelho, M. Santos, C. Viegas, Res. Microbiol. **166**, 557 (2015)
7. R. D. Scott, The direct medical costs of healthcare-associated infections in US hospitals and the benefits of prevention. http://www.cdc.gov/HAI/pdfs/hai/Scott_CostPaper.pdf. Accessed 4 Feb 2014
8. A. Jain, L.S. Duvvuri, S. Farah, N. Beyth, A.J. Domb, W. Khan, Adv. Healthc. Mater. **3**, 1969 (2014)
9. G. Yao, J. Lei, W. Zhang, C. Yu, Z. Sun, S. Zheng, Z. Sun, S. Zheng, S. Komarneni, Environ. Sci. Pollut. Res. **26**, 2782 (2019)
10. S.M. Dizaj, F. Lotfipour, M. Barzegar-Jalali, M.H. Zarrintan, K. Adibkia, Mater. Sci. Eng. C **44**, 278 (2014)
11. V.V. Kumar, S.P. Anthony, in *Surface Chemistry of Nanobiomaterials*, ed. by A.M. Grumezescu (Elsevier, Amsterdam, 2016), p. 265
12. C.-N. Lok, C.-M. Ho, R. Chen, Q.-Y. He, W.-Y. Yu, H. Sun, P.K.-H. Tam, J.-F. Chiu, C.-M. Che, J. Biol. Inorg. Chem. **12**, 527 (2007)
13. S. Chernousova, M. Epple, Angew. Chem. Int. Ed. **52**, 1636 (2013)
14. C. Marambio-Jones, E.M.V. Hoek, J. Nanoparticle Res. **12**, 1531 (2010)
15. L. Guo, W. Yuan, Z. Lu, C.M. Li, Colloids Surf. A **439**, 69 (2013)
16. G.A. Sotiriou, A. Teleki, A. Camenzind, F. Krumeich, A. Meyer, S. Panke, S.E. Pratsinis, Chem. Eng. J. **170**, 547 (2011)
17. M. Liong, B. France, K.A. Bradley, J.I. Zink, Adv. Mater. **21**, 1684 (2009)
18. R.N.M. Missengue, N.M. Musyoka, G. Madzivire, O. Babajide, O.O. Fatoba, M. Tuffin, L.F. Petrik, J. Environ. Sci. Health A **51**, 97 (2016)
19. N. Lubick, Environ. Sci. Technol. **42**, 8617 (2008)
20. H.-C. Zhou, S. Kitagawa, Chem. Soc. Rev. **43**, 5415 (2014)
21. H.-C. Zhou, J.R. Long, O.M. Yaghi, Chem. Rev. **112**, 673 (2012)
22. J.L.C. Rowsell, O.M. Yaghi, Microporous Mesoporous Mater **73**, 3 (2004)
23. J.-R. Li, R.J. Kuppler, H.-C. Zhou, Chem. Soc. Rev. **38**, 1477 (2009)
24. J. Lee, O.K. Farha, J. Roberts, K.A. Scheidt, S.T. Nguyen, J.T. Hupp, Chem. Soc. Rev. **38**, 1450 (2009)
25. L.E. Kreno, K. Leong, O.K. Farha, M. Allendorf, R.P. Van Duyne, J.T. Hupp, Chem. Rev. **112**, 1105 (2011)
26. P. Kumar, A. Deep, K.-H. Kim, TrAC. Trends Anal. Chem. **73**, 39 (2015)
27. P. Horcajada, T. Chalati, C. Serre, B. Gillet, C. Sebrie, T. Baati, J.F. Eubank, D. Heurtaux, P. Clayette, C. Kreuz, J.-S. Chang, Y.K. Hwang, V. Marsaud, P.-N. Bories, L. Cynober, S. Gil, G. Férey, P. Couvreur, R. Gref, Nat. Mater. **9**, 172 (2010)
28. E. Adatoz, A.K. Avci, S. Keskin, Sep. Purif. Technol. **152**, 207 (2015)
29. A. Argoub, R. Ghezini, C. Bachir, B. Boukoussa, A. Khelifa, A. Benguedach, P.G. Weidler, R. Hamacha, J. Porous Mater. **25**, 199 (2018)
30. S. Gwardiak, B. Szczęśniak, J. Choma, M. Jaroniec, J. Porous Mater. **26**, 775 (2019)
31. H. Jasuja, G.W. Peterson, J.B. Decoste, M.A. Browe, K.S. Walton, Chem. Eng. Sci. **124**, 118 (2015)
32. J.B. DeCoste, G.W. Peterson, Chem. Rev. **114**, 5695 (2014)
33. A.C. McKinlay, R.E. Morris, P. Horcajada, G. Férey, R. Gref, P. Couvreur, C. Serre, Angew. Chem. Int. Ed. **49**, 6260 (2010)
34. P. Horcajada, R. Gref, T. Baati, P.K. Allan, G. Maurin, P. Couvreur, G. Férey, R.E. Morris, C. Serre, Chem. Rev. **112**, 1232 (2011)
35. S. Aguado, J. Quirós, J. Canivet, D. Farrusseng, K. Boltes, R. Rosal, Chemosphere **113**, 188 (2014)
36. Y.-F. Guo, W.-J. Fang, J.-R. Fu, Y. Wu, J. Zheng, G.-Q. Gao, C. Chen, R.-W. Yan, S.-G. Huang, C.-C. Wang, Appl. Surf. Sci. **435**, 149 (2018)
37. G. Ximing, G. Bin, W. Yuanlin, G. Shuanghong, Mater. Sci. Eng. C **80**, 698 (2017)
38. T. Hu, Q. Jia, S. He, S. Shan, H. Su, Y. Zhi, L. He, J. Alloys Compd. **727**, 114 (2017)
39. S. Wang, L. Bromberg, H. Schreuder-Gibson, T.A. Hatton, ACS Appl. Mater. Interfaces **5**, 1269 (2013)
40. Y.K. Hwang, D. Hong, J. Chang, S.H. Jhung, Y. Seo, J. Kim, A. Vimont, M. Daturi, C. Serre, G. Férey, Angew. Chem. **120**, 4212 (2008)
41. N. Tian, Q. Jia, H. Su, Y. Zhi, A. Ma, J. Wu, S.Y. Shan, J. Porous Mater. **23**, 1269 (2016)

42. A. Samadi-Maybodi, S. Ghasemi, H. Ghaffari-Rad, Electrochim. Acta **163**, 280 (2015)
43. D. Rao, R. Lu, C. Xiao, E. Kan, K. Deng, Chem. Commun. **47**, 7698 (2011)
44. Q. Liang, M. Zhang, Z. Zhang, C. Liu, S. Xu, Z. Li, J. Alloys Compd. **690**, 123 (2017)
45. Y. Lin, C. Kong, L. Chen, RSC Adv. **6**, 32598 (2016)
46. N. Rani, A. Sharma, R. Singh, Mini. Rev. Med. Chem. **13**, 1812 (2013)
47. X. Guo, J. Shao, H. Liu, B. Chen, W. Chen, Y. Yu, RSC Adv. **5**, 51559 (2015)
48. J. Pandey, V.K. Tiwari, S.S. Verma, V. Chaturvedi, S. Bhatnagar, S. Sinha, A.N. Gaikwad, P.R. Tripathia, Eur. J. Med. Chem. **44**, 3350 (2009)
49. E. Eisbein, J.-O. Joswig, G. Seifert, Microporous Mesoporous Mater. **216**, 36 (2015)
50. S. Liu, Z. Yue, Y. Liu, Dalt. Trans. **44**, 12976 (2015)
51. F.-M. Zhang, L.-Z. Dong, J.-S. Qin, W. Guan, J. Liu, S.-L. Li, M. Lu, Y.-Q. Lan, Z.-M. Su, H.-C. Zhou, J. Am. Chem. Soc. **139**, 6183 (2017)
52. J. Li, T. Qi, L. Wang, C. Liu, Y. Zhang, Mater. Lett. **61**, 3197 (2007)
53. A. Abbaszadegan, Y. Ghahramani, A. Gholami, B. Hemmateenejad, S. Dorostkar, M. Nabavizadeh, H. Sharghi, J. Nanomater. **16**, 53 (2015)
54. S.A.M. Hanim, N.A.N.N. Malek, Z. Ibrahim, Vacuum **143**, 344 (2017)
55. T.C. Dakal, A. Kumar, R.S. Majumdar, V. Yadav, Front. Microbiol. **7**, 1831 (2016)
56. L. Bromberg, Y. Diao, H. Wu, S.A. Speakman, T.A. Hatton, Chem. Mater. **24**, 1664 (2012)
57. N. Cao, S. Tan, W. Luo, K. Hu, G. Cheng, Catal. Lett. **146**, 518 (2016)
58. https://clsi.org/standards/products/microbiology/documents/m100
59. S. Bykkam, M. Ahmadipour, S. Narisngam, V.R. Kalagadda, S.C. Chidurala, Adv. Nanopart. **4**, 1 (2015)
60. I.A. Wani, S. Khatoon, A. Ganguly, J. Ahmed, A.K. Ganguli, T. Ahmad, Mater. Res. Bull. **45**, 1033 (2010)
61. M. Shafiei, M.S. Alivand, A. Rashidi, A. Samimi, D. Mohebbi-Kalhori, Chem. Eng. J. **341**, 164 (2018)
62. A.B. Rostam, M. Peyravi, M. Ghorbani, M. Jahanshahi, Appl. Surf. Sci. **427**, 17 (2018)
63. M.B. Boroujeni, A. Hashemzadeh, M.-T. Faroughi, A. Shaabani, M.M. Amini, RSC Adv. **6**, 100195 (2016)
64. Z. Sun, C. Fan, X. Tang, J. Zhao, Y. Song, Z. Shao, L. Xu, Appl. Surf. Sci. **387**, 828 (2016)
65. http://www.who.int/water_sanitation_health/dwq/chemicals/silver.pdf
66. www.cdc.gov/niosh-rtecs/NI32BC48.html
67. https://www.who.int/water_sanitation_health/dwq/…/chromium.pdf
68. https://www.epa.gov/dwstandardsregulations/chromium-drinking-water
69. G. Ferey, C. Mellot-Draznieks, C. Serre, F. Millange, J. Dutour, S. Surble, I. Margiolaki, Science **309**, 2040 (2005)
70. H.E. Emam, O.M. Darwesh, R.M. Abdelhameed, Colloids Surf. B **165**, 219 (2018)
71. K. Shameli, M. Bin Ahmad, M. Zargar, W.M.Z.W. Yunus, N.A. Ibrahim, Int. J. Nanomed. **6**, 331 (2011)
72. L. Ferreira, J.F. Guedes, C. Almeida-Aguiar, A.M. Fonseca, I.C. Neves, Colloids Surf. B **142**, 141 (2016)
73. L. Ferreira, A.M. Fonseca, G. Botelho, C. Almeida-Aguiar, I.C. Neves, Microporous Mesoporous Mater. **160**, 126 (2012)
74. X. Lu, J. Ye, D. Zhang, R. Xie, R. FeyisBogale, Y. Suna, L. Zhaoa, Q. Zhao, G. Ning, J. Inorg. Biochem. **138**, 114 (2014)
75. B. Mortada, T.A. Matar, A. Sakaya, H. Atallah, Z. KaraAli, P. Karam, M. Hmadeh, Inorg. Chem. **56**, 4739 (2017)
76. M. Berchel, T.L. Gall, C. Denis, S.L. Hir, F. Quentel, C. Elléouet, T. Montier, J.-M. Rueff, J.-Y. Salaün, J.-P. Haelters, G.B. Hix, P. Lehnb, P.-A. Jaffrès, New J. Chem. **35**, 1000 (2011)
77. G. Wyszogrodzka, B. Marszałek, B. Gil, P. Dorożyński, Drug. Discov. Today **21**, 1009 (2016)
78. M. Moritz, M. Geszke-Moritz, Chem. Eng. J. **228**, 596 (2013)
79. J.S. Kim, E. Kuk, K.N. Yu, J.H. Kim, S.J. Park, H.J. Lee, S.H. Kim, Y.K. Park, Y.H. Park, C.Y. Hwang, P.K. Kim, Y.S. Lee, D.H. Jeong, M.H. Cho, Nanomed. Nanotechnol. Biol. Med. **3**, 95 (2007)
80. S. Shrivastava, T. Bera, A. Roy, G. Singh, P. Ramachandrarao, D. Dash, Nanotechnology **18**, 225103 (2007)
81. S.A.M. Hanim, N.A.N.N. Malek, Z. Ibrahim, Appl. Surf. Sci. **360**, 121 (2016)